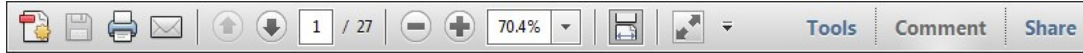
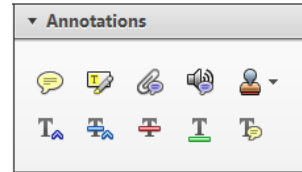


Once you have Acrobat Reader open on your computer, click on the [Comment](#) tab at the right of the toolbar:



This will open up a panel down the right side of the document. The majority of tools you will use for annotating your proof will be in the [Annotations](#) section, pictured opposite. We've picked out some of these tools below:



### 1. Replace (Ins) Tool – for replacing text.

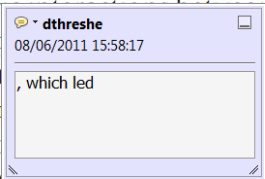


Strikes a line through text and opens up a text box where replacement text can be entered.

#### How to use it

- Highlight a word or sentence.
- Click on the [Replace \(Ins\)](#) icon in the Annotations section.
- Type the replacement text into the blue box that appears.

standard framework for the analysis of microeconomic activity. Nevertheless, it also led to the development of a number of strategic approaches to the analysis of the number of competitors in an industry. This is that the strategic components of the main components of the industry level, are exogenous to the industry. An important work on this by Shirasaka (1987) henceforth) we open the 'black b



### 2. Strikethrough (Del) Tool – for deleting text.



Strikes a red line through text that is to be deleted.

#### How to use it

- Highlight a word or sentence.
- Click on the [Strikethrough \(Del\)](#) icon in the Annotations section.

there is no room for extra profits as mark-ups are zero and the number of firms (net) values are not determined by market structure. Blanchard and ~~Kiyotaki~~ (1987), perfect competition in general equilibrium. The effects of aggregate demand and supply shocks in a classical framework assuming monopolistic competition and an exogenous number of firms

### 3. Add note to text Tool – for highlighting a section to be changed to bold or italic.



Highlights text in yellow and opens up a text box where comments can be entered.

#### How to use it

- Highlight the relevant section of text.
- Click on the [Add note to text](#) icon in the Annotations section.
- Type instruction on what should be changed regarding the text into the yellow box that appears.

dynamic responses of mark-ups consistent with the VAR evidence

sation by Markov and Bellotti (2008) and on the number of competitors in the industry. It is that the structure of the sector is also consistent with the demand-



### 4. Add sticky note Tool – for making notes at specific points in the text.



Marks a point in the proof where a comment needs to be highlighted.

#### How to use it

- Click on the [Add sticky note](#) icon in the Annotations section.
- Click at the point in the proof where the comment should be inserted.
- Type the comment into the yellow box that appears.

and supply shocks. Most of the empirical evidence on the dynamic responses of mark-ups is consistent with the VAR evidence. The standard framework for the analysis of the number of competitors and the impact of aggregate demand and supply shocks is that the structure of the sector



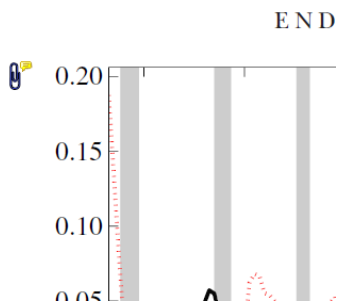
5. **Attach File** Tool – for inserting large amounts of text or replacement figures.



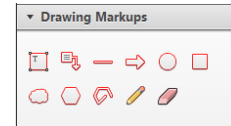
Inserts an icon linking to the attached file in the appropriate place in the text.

How to use it

- Click on the **Attach File** icon in the Annotations section.
- Click on the proof to where you'd like the attached file to be linked.
- Select the file to be attached from your computer or network.
- Select the colour and type of icon that will appear in the proof. Click OK.

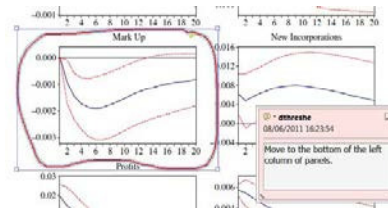


6. **Drawing Markups** Tools – for drawing shapes, lines and freeform annotations on proofs and commenting on these marks. Allows shapes, lines and freeform annotations to be drawn on proofs and for comment to be made on these marks.



How to use it

- Click on one of the shapes in the Drawing Markups section.
- Click on the proof at the relevant point and draw the selected shape with the cursor.
- To add a comment to the drawn shape, move the cursor over the shape until an arrowhead appears.
- Double click on the shape and type any text in the red box that appears.



ORIGINAL  
ARTICLE

# S100 $\beta$ as an early biomarker of excitotoxic damage in spinal cord organotypic cultures

Graciela L. Mazzone<sup>1</sup> and Andrea Nistri

Neuroscience Department, International School for Advanced Studies (SISSA), Trieste, Italy

**Abstract**

~~Astroglial calcium-binding protein~~ (S100 $\beta$ ) is a cytoplasmic calcium-binding protein mainly expressed by glia and considered to be a useful biomarker for brain or spinal cord injury. Indeed, clinical studies suggest that the S100 $\beta$  concentration in serum or cerebrospinal fluid may predict lesion outcome and prognosis. The relation of S100 $\beta$  levels to damage severity and its timecourse remains, however, unclear. This study used a validated *in vitro* model of spinal cord injury induced by kainate-mediated excitotoxicity to investigate these issues. After 22 days *in vitro*, rat organotypic spinal cord slices were subjected to one transient application (1 h) of 1 or 100  $\mu$ M kainate followed by washout. While the lower kainate concentration did not evoke neuronal loss or S100 $\beta$  increase, the larger concentration elicited 40% neuronal death, no change in glial number and a delayed, significant rise in extracellular

S100 $\beta$  that peaked at 24 h. This increase was associated with a stronger expression of the S100 $\beta$  protein as indicated by western blotting and immunohistochemistry. Application of the microtubule disrupting agent colchicine did not change the rise in S100 $\beta$  induced by kainate, an effect blocked by the glutamate receptor antagonists CNQX and APV. Our data suggest that excitotoxicity was followed by release of S100 $\beta$  perhaps from a readily releasable pool through a mechanism independent of microtubule assembly. The raised extracellular level of S100 $\beta$  appeared to reflect glial reactivity to the kainate-evoked lesion in accordance with the view that this protein may be involved in tissue protection and repair after acute injury.

**Keywords:** colchicine, glutamate receptor, kainic acid, neuroprotection, spinal cord injury.

*J. Neurochem.* (2014) 10.1111/jnc.12748

Management of acute brain or spinal injury requires monitoring of early damage progression to direct treatment and predict outcome (Gentleman 1999). In this framework, the availability of soluble biomarkers represents an important goal. Recently, astroglial calcium-binding protein (S100 $\beta$ ), a calcium-binding protein with tissue-specific expression (Michetti *et al.* 2012), has been reported to be significantly increased in serum or cerebrospinal fluid after experimental or clinical spinal cord injury (SCI) (Cao *et al.* 2008; Kwon *et al.* 2010), and to be related to the lesion severity even if the precise link between S100 $\beta$  and neuronal and/or glial damage, and the S100 $\beta$  time profile are poorly understood. Although serum S100 $\beta$  concentration increases after traumatic brain injury (Yokobori *et al.* 2013), its relation to the damage severity and prognosis also remains controversial (Mercier *et al.* 2013). In the nervous system, S100 $\beta$  is produced, stored, and released mainly from astrocytes and Schwann cells (even though its family member S100A1 can be observed in a few neurons), and is viewed to play an important role in neurorepair and regeneration mechanisms (Michetti *et al.* 2012). The origin of extracellular S100 $\beta$  may be from damaged cells as well

as via secretion through a Golgi-independent pathway (Donato *et al.* 2013).

The principal feature of acute SCI pathophysiology is excitotoxicity that is considered the main contributor to the clinical outcome (Schwab *et al.* 2006; Rowland *et al.* 2008; Mehta *et al.* 2013). Our *in vitro* SCI model using excitotoxic damage evoked by transient kainate application to organotypic slice cultures (with predominant neuro- rather than

Received March 19, 2014; revised manuscript received April 16, 2014; accepted April 23, 2014.

Address correspondence and reprint requests to Andrea Nistri, SISSA, Via Bonomea 265, 34136 Trieste, Italy. E-mail: nistri@sisssa.it

<sup>1</sup>Present address: Laboratorios de Investigación aplicada en Neurociencias (LIAN) - Fundación para la Lucha contra las Enfermedades Neurológicas de la Infancia (FLENI), Escobar, Buenos Aires, Argentina and CONICET, Buenos Aires, Argentina.

*Abbreviations used:* CNQX, 6-cyano-7-nitroquinoxaline-2, 3-dione; Ctrl, control; DAPI, 4',6-diamidino-2-phenylindole; D-APV, D-amino-phosphonoveralate; DIV, days *in vitro*; DME/HIGH, Dulbecco's modified Eagle's medium high glucose; FCS, fetal calf serum; GFAP, glial fibrillary acidic protein; KA, kainate; NeuN, neuronal specific nuclear protein; NGF, nerve growth factor; S100 $\beta$ , astroglial calcium-binding protein S100 $\beta$ ; SCI, spinal cord injury.

glio-toxicity) closely mimics the *in vivo* pathophysiology of SCI by producing neuronal loss fully manifested 24 h later with minimal damage to astrocytes (Mazzone and Nistri 2010; Mazzone *et al.* 2013). Thus, using the excitotoxic model of organotypic spinal slices, the aim of this study was to characterize the expression and extracellular concentration of S100 $\beta$  in relation to neuronal damage, and its timecourse.

## Materials and methods

### Preparation and maintenance of organotypic cultures

Organotypic slice cultures from Wistar rat (supplied by Harlan Laboratories, S. Giovanni al Natisone, UD, Italy) embryos of both sexes (Mazzone and Nistri 2010; Mazzone *et al.* 2010) were prepared in accordance with the guidelines approved by the Scuola Internazionale Superiore di Studi Avanzati (Trieste) Ethical Committee: all efforts were made to minimize suffering and number of animals used. Culture slices were grown for 22 days *in vitro* (DIV) in a complete medium containing 82% Dulbecco's Modified Eagle medium (DME/HIGH; osmolarity 300 mOsm, pH 7.35), 8% sterile water, 10% fetal bovine serum (Invitrogen, Milano, Italy), 5 ng/mL nerve growth factor (Alomone Laboratories; Jerusalem, Israel) following standard procedures (Spenger *et al.* 1991; Streit *et al.* 1991).

### Excitotoxic injury on organotypic cultures

At 22 DIV excitotoxicity injury was produced by application of kainate for 1 h (100  $\mu$ M; Ascent Scientific, Bristol, UK) dissolved in complete culture medium and then carefully washed out with complete medium. In a few tests 1  $\mu$ M kainate was used. In each experiment control sister cultures (sham) were untreated and maintained *in vitro* for the same time points and subjected to the same medium washout. The glutamate receptor antagonists CNQX (20  $\mu$ M; Tocris, Bristol, UK) and D-aminophosphonovaleate (50  $\mu$ M; Tocris) were used as previously reported (Margaryan *et al.* 2010). To block the S100 $\beta$  secretion pathway owing to microtubule depolymerization, colchicine (Sigma, Milan, Italy) was used at 12  $\mu$ M (5  $\mu$ g/mL) and 62.6  $\mu$ M (25  $\mu$ g/mL) concentration.

### Organotypic slice immunostaining and cell counting

Immunohistochemistry experiments were performed as detailed recently (Cifra *et al.* 2012). Cryoprotected slices were incubated with the previously validated primary antibodies NeuN (1 : 250; Millipore, Billerica, MA, USA), or S100 $\beta$  (1 : 1000; Dako, Glostrup, Denmark). The primary antibody was visualized using a secondary fluorescent antibody (Alexa Fluor 488 or 594 at 1 : 500 dilution, Invitrogen, Carlsbad, CA, USA). To visualize cell nuclei, slices were incubated with 4', 6-diamidino-2-phenylindole (DAPI, 1  $\mu$ g/mL; Sigma). For each slice culture, the number of NeuN positive cells was obtained by counting stacks of 25–30 images with a confocal microscope as previously described (Mazzone *et al.* 2010; Cifra *et al.* 2012). The number of NeuN positive cells was quantified with 'eCELLence' software (Glance Vision Tech, Trieste, Italy). The S100 $\beta$  signals were collected as mean fluorescence intensity with densitometry analysis using a Zeiss Axioskop2 microscope and MetaVue software (Molecular Devices, Sunnyvale, CA, USA). DAPI nuclear staining was used to identify the dead or dying cells quantified with 'eCELLence' software as previously

reported (Mazzone *et al.* 2010). The average percent values of nuclei with condensed chromatin were compared between control- and kainate-treated slices and normalized to the total number of nuclei.

### S100 $\beta$ ELISA assay

S100 $\beta$  was measured with a commercially available kit (BioVendor, Brno, Czech Republic) following the manufacturer's indications. This test measures human S100 $\beta$ , validated for rat S100 $\beta$ , with no detectable crossreactivity to human S100A1, S100P, S100 Z, and neuroglobin; approximately 2% crossreactivity to human glial fibrillary acidic protein (GFAP) was observed. The sensitivity of the assay is 15 pg/mL. To exclude interference owing to culture conditions, blanks of complete medium and with the kit dilution buffer were tested and gave similar basal absorbance levels. Samples to the microtiter plate wells were incubated for 2 h at 25°C and processed in accordance with the manufacturer's instructions (<http://www.biovendor.com/product/immunoassays/s100b-human-elisa>). The sample absorbance was measured spectrophotometrically, at 450 nm and 620 nm wavelength, with a microplate reader (Thermo Scientific Multiskan FC microplate photometer, Thermo Scientific Oy, Vantaa, Finland). The concentration of S100 in the samples was calculated by comparing the optical density of the samples to the standard curve, using the microplate accompanying reader software and by using a four-parameter algorithm calculation (<http://www.shibayagi.co.jp>). We also validated our assay by adding to blank samples 300 pg/mL of S100 $\beta$  for 24 h and measured the protein concentration recovery which was  $71 \pm 1.4\%$  ( $n = 4$ ).

### S100 $\beta$ western blotting

Organotypic slices were placed on ice and disrupted with lysis buffer (50 mM Tris-HCl pH 8, 150 mM NaCl, 1 mM EDTA, 0.1% sodium dodecyl sulfate, 1% Igepal CA-630, 4% v/v protease inhibitor cocktail (Roche Applied Science, Penzberg, Germany), 0.5% sodium deoxycholate) by sonication (Sanyo MSE Soniprep 150, MSE Ltd, London, UK) two times for 15 s. Protein concentration in the lysate was determined by bicinchoninic acid protein assay following the manufacturer's instructions (B-9643, Sigma). Equal amounts of protein (25  $\mu$ g) were separated on sodium dodecyl sulfate polyacrylamide gel (17.5%) with electrophoresis using  $\beta$ -mercaptoethanol for 1.5 h at 150 V. As a size standard, Page Ruler Prestained Protein Ladder (Fisher Scientific SAS, Illkirch Cedex, France) from 10 kDa to 170 kDa was used. Proteins were transferred onto a nitrocellulose membrane for 1 h (80 mV) at room temperature, followed by overnight transfer (15 mV) at 4°C. Membranes were incubated in 5% milk/phosphate-buffered saline with 0.1% Tween-20 with primary anti-S100 $\beta$  antibody (1 : 2000; Dako) or GFAP mouse monoclonal anti-GFAP (1 : 2000; Sigma) followed by horseradish peroxidase-conjugated secondary antibody for 2 h at 25°C. Immunoreactive protein bands were then visualized with enhanced chemiluminescence (Amersham Biosciences). Membranes were successively incubated with a stripping buffer (0.5 mM Tris/HCl pH 6.8, 0.2% v/v sodium dodecyl sulfate, 0.68% v/v  $\beta$ -mercaptoethanol) for 30 min at 55°C before incubation with  $\beta$ -actin horseradish peroxidase conjugated (1 : 5000; Sigma). Data acquired using Alliance LD2-77WL (Uvitec, Cambridge, UK) were analyzed with Uviband software (Uvitec) and normalized to GFAP (utilized as loading control). As shown in

Fig. 2a, GFAP immunoblotting showed a 50 kDa band and smaller ones as reported (Wang and Hatton 2009; Roybon *et al.* 2013).

### Statistical analysis

Data represent mean  $\pm$  SEM where  $n$  refers to the number of organotypic cultures slices. Statistical calculations were done using SigmaStat 3.11 (Systat Software, Chicago, IL, USA). For multiple comparisons the ANOVA test for parametric data was used, followed by the Tukey–Kramer *post hoc* test or *t*-tests for comparisons between two different groups. Non-parametric values were analyzed with the Kruskal–Wallis test or the Mann–Whitney Rank Sum Test.  $p \leq 0.05$  was regarded as statistically significant.

## Results

Figure 1a and c show that, in control conditions, the S100 $\beta$  fluorescence strength did not change over extended (up to

336 h) culturing *in vitro* (time 0 h corresponds to 22 DIV). After kainate application, the S100 $\beta$  immunosignal rose to reach a significantly-high peak 72 h later with slow return toward control at 336 h. Fig. 1b<sub>1</sub> shows typical staining of neurons (NeuN positive cells) before or after kainate treatment with substantial loss (see also grey line in Fig. 1d) leaving  $60 \pm 4\%$  neurons 24 h later ( $n = 6$ ). As indicated in the plot of Fig. 1d, the number of neurons stabilized at 24 h in correspondence with the peak in the number of pyknotic cells (stained with DAPI as exemplified in Fig. 1b<sub>1-2</sub>; black curve in Fig. 1d) in accordance with a recent report (Mazzone *et al.* 2013). These observations indicate that there was substantial time lag between neuronal loss and increase in intracellular S100 $\beta$  signal strength.

To further investigate this phenomenon, we studied if the enhanced S100 $\beta$  immunoreactivity might have been owing

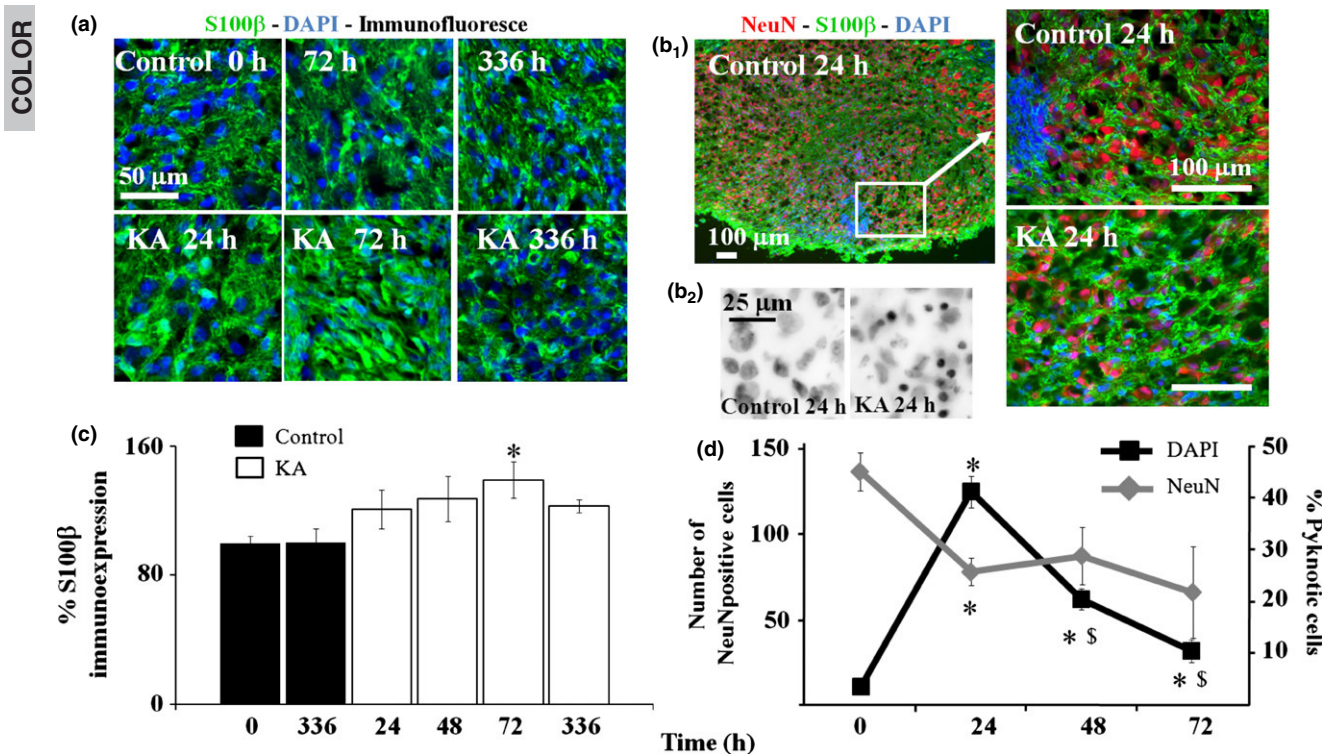


**Fig. 1** Astroglial calcium-binding protein (S100 $\beta$ ) in relation to cell death evoked by kainate. (a) Representative staining of S100 $\beta$  (green) and 4',6-diamidino-2-phenylindole (DAPI) (blue) positive cells for spinal tissue at 0 (22 DIV), 72 or 336 h in control conditions (upper panels) or after kainate (KA) treatment (lower panels). (b<sub>1</sub>) Representative NeuN (red), S100 $\beta$  (green) and DAPI-positive (blue) positive cells in control condition (24 h; see also inset on the right at higher magnification) or 24 h after kainate application (bottom right; note loss of NeuN positive elements). The examples in b<sub>2</sub> show control DAPI nuclear staining (left) and pyknotic nuclei (right) following kainate application. (c) Histograms show increase in S100 $\beta$  mean fluorescence intensity expressed as percent of control at 72 h after kainate ( $n = 3$ –12 slices, from at least two different experiments,  $*p = 0.003$

vs. control). Note increased S100 signal in kainate-treated slices at 72 h but not 24, 48 or 336 h. S100 $\beta$  immunostaining was quantified (with densitometry analysis of a  $500 \times 500 \mu\text{m}$  area) to provide mean data for at least two experiments in which 3–12 slices were used. (d) Plots showing the number of NeuN positive cells (grey diamonds; left scale) in the dorsal horn counted before kainate application and 24, 48, and 72 h after kainate ( $100 \mu\text{M}$  for 1 h). At these time points, surviving neurons were 60, 60, and 51%, respectively, of the control neuronal population (taken at zero time). In parallel, there was a significant increase in the percent of pyknotic nuclei (filled squares; right scale) peaking at 24 h, and decreasing 48 and 72 h later.  $*p < 0.05$  versus time 0 (control condition at 22 DIV),  $^{\$}p < 0.05$  versus 24 h kainate ( $n = 6$ ).

to raised protein expression. The western blot experiments (see examples in Fig. 2a) demonstrated a statistically significant rise in the S100 $\beta$  protein level 24 h after kainate (Fig. 2c;  $p = 0.042$ ). Fig. 2b shows a calibration gel done by loading different quantities of protein (from 50 to 3.12  $\mu\text{g}$  of total protein) from sham spinal cords and also from embryo samples (13 day of gestation; 25  $\mu\text{g}$  of total protein per well), the latter known to lack S100 $\beta$  (Roybon *et al.* 2013). We could, therefore, estimate the effective amount of S100 $\beta$  and GFAP present in our cultures by plotting the gel band density versus the quantity of loaded protein as a strong linear relation was found ( $R^2 = 0.9995$  for S100 $\beta$ ,  $R^2 = 0.911$  for GFAP;  $n = 2-4$  gels with 5-10 slices). These data demonstrated that, after 24 h, cultures expressed  $0.156 \pm 0.020$   $\mu\text{g}$  or  $0.433 \pm 0.0263$   $\mu\text{g}$  of S100 $\beta$ /GFAP in control condition or after kainate, respectively ( $p \leq 0.001$ ;  $n = 4-5$ ).

The protein levels cannot, however, be predictive for the quantity of the S100 $\beta$  in the cell medium that was studied

with an ELISA assay. Fig. 2d shows that, in control condition medium, repeated washouts over 24 h led to a slow, self-limited rise in S100 $\beta$  (black line) presumably owing to the culture medium change (Ellis *et al.* 2007; Gyorgy *et al.* 2011) and without further increase at later time. Immediately at the end of kainate treatment (grey line in Fig. 2d), the level of S100 $\beta$  was undetectable, indicating the acute excitotoxicity was not accompanied by a significant amount of extracellular S100 $\beta$ . Nevertheless, extracellular S100 $\beta$  concentration slowly grew and, after 24 h following kainate washout, was significantly increased ( $p = 0.033$ ) with decline over the subsequent 2-3 days. Application of 1  $\mu\text{M}$  kainate (1 h) that is known to yield minimal damage (Mazzone *et al.* 2010), did not evoke a significant change in S100 $\beta$  levels after 24 h washout ( $14.6 \pm 3.2$  pg/mg cell protein in control vs.  $11.2 \pm 2.4$  pg/ mg cell protein after kainate,  $n = 4$  slices).

Recent evidence indicates that, following brain injury, S100 $\beta$  may not simply leak out from damaged cells, but it is

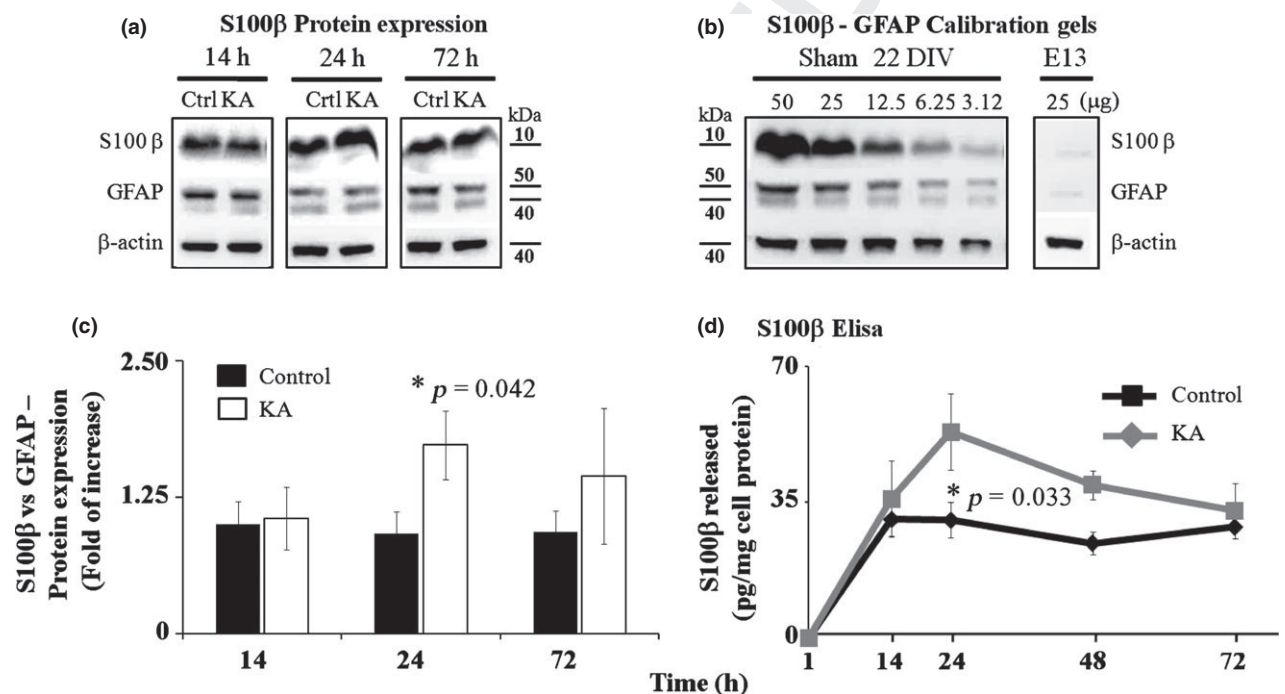


**Fig. 2** Time-dependent effect of kainate on astroglial calcium-binding protein (S100 $\beta$ ). (a) S100 $\beta$  western blot analysis using organotypic slices treated for 14, 24 or 72 h with or without kainate (100  $\mu\text{M}$  for 1 h). In each lane, 25  $\mu\text{g}$  of protein was loaded, and membranes were probed with S100 $\beta$  (upper line), glial fibrillary acidic protein (GFAP) (middle line; note double GFAP band as described by Wang and Hatton 2009; Roybon *et al.* 2013) and  $\beta$ -actin (lower line) antibodies. Note the significant increase in the S100 $\beta$  protein levels 24 h after kainate. (b) Calibration experiment using sham cultures (22 DIV): in each lane different protein concentrations were loaded (from 50 to 3.12  $\mu\text{g}$ ). A linear relation between amount of loaded protein and densitometry signal was obtained for quantitative analysis ( $R^2 = 0.9995$  for S100 $\beta$

and 0.911 for GFAP;  $n = 2-4$ ). Right panel shows expression level of S100 $\beta$ , GFAP and  $\beta$ -actin in embryos (at 13 days of gestation) using 25  $\mu\text{g}$  load. Note absence of S100 $\beta$  and GFAP at this time of gestation in accordance with Roybon *et al.* (2013). (c) Histograms show densitometry analysis of S100 $\beta$  expression normalized to the density of GFAP (each band was analyzed with Uviband software). Values are referred to a fractional change versus untreated controls. \* $p < 0.042$  versus control,  $n = 6-9$ . (d) Plots of S100 $\beta$  levels in supernatants measured with ELISA assay for slices in control conditions or 14, 24 or 72 h after kainate treatment. Note the significant increase at 24 h after kainate. Data represent mean values  $\pm$  SEM of at least three different experiments, \* $p = 0.033$  versus control;  $n = 3-11$ .

also actively secreted via a cytoskeleton process that includes vesicle translocation and/or exocytosis (Davey *et al.* 2001; Donato *et al.* 2013). In order to clarify this issue, we treated our cultures with the microtubule disruptor colchicine (Sorci *et al.* 1998) that depolymerizes vesicular transport and causes vesicle accumulation in the cell soma. Fig. 3a shows nuclear staining for control conditions (left panel) or after 24 h colchicine (12 or 62.6  $\mu$ M, middle and right panels). Significant increase in aberrant nuclear morphology was found with the higher colchicine dose (62.6  $\mu$ M,  $p < 0.05$ ;  $n = 3$ ; Fig. 3c) and led us to use the 12  $\mu$ M concentration that altered cell morphology without inducing significant cell death (see example in Fig. 3b). Organotypic cultures were, therefore, treated (1 h) with kainate plus 12  $\mu$ M colchicine that was left in the medium up to the observation time-point. Fig. 3d shows that the strong rise in extracellular S100 $\beta$  evoked by kainate was prevented by co-application of CNQX (20  $\mu$ M) plus D-AVP<sub>1</sub> (50  $\mu$ M), demonstrating the process dependence on glutamate receptor activity, and was not inhibited when kainate was co-applied with 12  $\mu$ M

colchicine, alluding to alternative pathways for S100 $\beta$  release independent from microtubule assembly.

## Discussion

This report shows that, in this model, excitotoxicity was associated with about 40% neuronal death. This paradigm was not accompanied by glial loss evaluated with GFAP western blotting (Fig. 2a), a finding in accordance with previous studies (Kuzhandaivel *et al.* 2010), and was characterized by a strong rise in extracellular S100 $\beta$  within the first 24 h. Furthermore, glial expression of the same protein was enhanced, whereas the medium concentration of this protein gradually fell. These data are consistent with the early rise in serum S100 $\beta$  observed in the spinal cord *in vivo* following acute contusion (Cao *et al.* 2008) even if the histological damage had not been quantified. Likewise, a large clinical study detected the maximum level of CSF S100 $\beta$  24 h after the primary SCI (Kwon *et al.* 2010). In the rabbit spinal cord subjected to repeated compressive

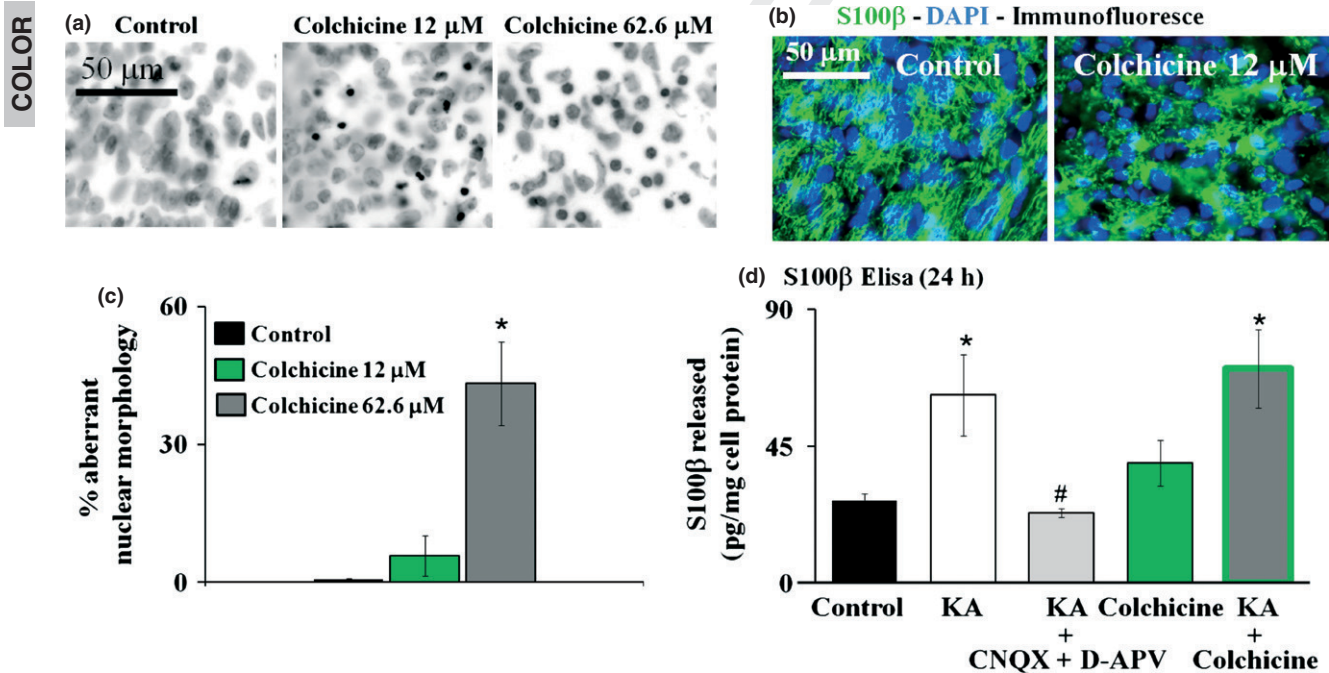


**Fig. 3** Modulation of extracellular astroglial calcium-binding protein (S100 $\beta$ ) level induced by kainate. (a) Examples of nuclear staining with 4',6-diamidino-2-phenylindole (DAPI) in control condition (left) or after 24 h application of colchicine (12  $\mu$ M, middle panel; 62.6  $\mu$ M, right panel). Note that the higher dose of colchicine increased occurrence of aberrant nuclear morphology. (b) Representative S100 $\beta$  (green) and DAPI (blue) positive cells in control condition or after 24 h application colchicine (12  $\mu$ M). Note large change in cell morphology after colchicine application. (c) Histograms showing the percent values of aberrant nuclear morphology at 24 h after colchicine application (12  $\mu$ M, open bar; 62.6  $\mu$ M, grey bar).

\* $p < 0.05$  versus controls (untreated cultures, filled bar,  $n = 2-3$  slices). (d) S100 $\beta$  levels in supernatants measured with ELISA assay for slices in control conditions, 24 h after washout of kainate alone (100  $\mu$ M for 1 h), or co-applied with CNQX (20  $\mu$ M) plus D-AVP<sub>1</sub> (50  $\mu$ M) or with colchicine (12  $\mu$ M). CNQX plus D-APV or colchicine were also continuously applied during the washout phase. Note a significant increase in S100 $\beta$  levels was prevented by CNQX plus APV. Colchicine (12  $\mu$ M) did not block S100 $\beta$  release. Data represent mean values  $\pm$  SEM of two different experiments, \* $p < 0.05$  versus control,  $n = 3-11$  slices; # $p = 0.005$  versus kainate,  $n = 4-11$  slices.

challenges over an extended timeframe, the serum S100 $\beta$  was elevated in relation to the global cell loss and degree of paralysis (Marquardt *et al.* 2011). All these investigations leave, however, unclear the source and timecourse of extracellular S100 $\beta$ .

In this study, excitotoxicity was the primary process to trigger S100 $\beta$  liberation as pharmacological block of ionotropic glutamate receptors prevented any increment in the S100 $\beta$  levels. We have previously shown that kainate stimulation is a trigger to induce delayed neuronal death primarily via a non-apoptotic process developing over several hours (Kuzhandaivel *et al.* 2011), rather than producing rapid necrosis which is a less intense process with very early rise in medium LDH levels (Mazzone *et al.* 2010; Mazzone and Nistri 2011). Importantly, we have observed no significant increment in S100 $\beta$  when kainate was applied at 1  $\mu$ M depolarizing concentration known to be unable to evoke excitotoxicity (Mazzone *et al.* 2010). Beyond the 24 h time-point from kainate washout, neuronal losses stabilized together with return of S100 $\beta$  levels toward baseline. Thus, the simplest interpretation is that extracellular S100 $\beta$  levels probably reflect ongoing neuronal damage rather than representing a marker of former cell damage. Previous studies have indicated the dual nature of the S100 $\beta$  effects, namely trophic at low concentration and toxic at a high one (Michetti *et al.* 2012). The S100 $\beta$  levels detected in this study place the protein concentration in the first category.

Although S100 $\beta$  is mainly expressed by glial cells (Michetti *et al.* 2012), a few neurons can express members of the S100 protein family, especially S100A1 (Rickmann and Wolff 1995), which is not recognized by the antibody used in this study. *In vitro* studies of rat brain primary cultures have indicated that, after mechanical injury, S100B is primarily and most abundantly released by glia (Ellis *et al.* 2007). These data, therefore, suggest that, after kainate application, S100 $\beta$  was released predominantly by glia little damaged by the excitotoxic stimulation. On organotypic cerebellar cultures, long-lasting application of unconjugated bilirubin induces excitotoxic stress primarily affecting oligodendrocytes with enhanced astrocyte GFAP immunostaining and with no significant rise in extracellular S100 $\beta$  (Barateiro *et al.* 2014): the different results between cerebellar and spinal networks indicate that S100 $\beta$  levels are likely related to the regional distribution of the excitotoxic damage and its cell targets. Members of the S100 family are thought to be released via a microtubule-dependent pathway (Davey *et al.* 2001) that is inhibited by colchicine (Rammes *et al.* 1997). The mechanism for S100 $\beta$  release detected in this study remains unclear as it was not prevented by colchicine. One might surmise that excitotoxicity triggered S100 $\beta$  release from a readily releasable pool of this protein and that this phenomenon subsequently stimulated a lasting increase in protein expression.

In conclusion, an *in vitro* model of SCI using organotypic slices that retain the basal network organization, indicates that, after an excitotoxic stimulus, extracellular S100 $\beta$  was significantly elevated in association with ongoing neuronal damage and unscathed glia. It is likely that the S100 $\beta$  level is a biomarker for glial reactivity to lesion and accords with the proposal that S100 $\beta$  plays an important role in early neuroprotection processes (Sorci *et al.* 2013).

## Acknowledgment and conflict of interest disclosure

We thank Dr. Beatrice Pastore for her assistance with organotypic cultures. This study was supported by the European Fund for CrossBorder Cooperation (MINA project) between Italy and Slovenia. The authors declare no conflicts of interest.

All experiments were conducted in compliance with the ARRIVE guidelines.

## References

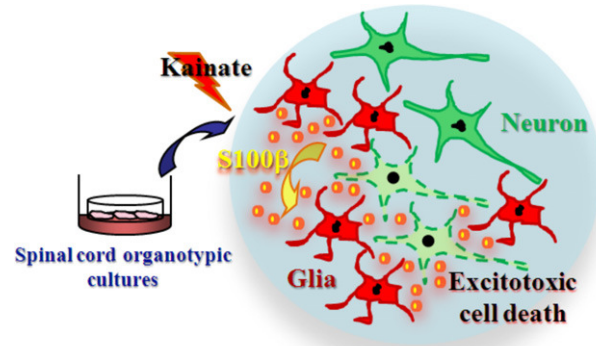
- Barateiro A., Domingues H. S., Fernandes A., Relvas J. B. and Brites D. (2014) Rat cerebellar slice cultures exposed to bilirubin evidence reactive gliosis, excitotoxicity and impaired myelinogenesis that is prevented by AMPA and TNF- $\alpha$  inhibitors. *Mol. Neurobiol.* **49**, 424–439.
- Cao F., Yang X. F., Liu W. G., Hu W. W., Li G., Zheng X. J., Shen F., Zhao X. Q. and Lv S. T. (2008) Elevation of neuron-specific enolase and S-100beta protein level in experimental acute spinal cord injury. *J. Clin. Neurosci.* **15**, 541–544.
- Cifra A., Mazzone G. L., Nani F., Nistri A. and Mladinic M. (2012) Postnatal developmental profile of neurons and glia in motor nuclei of the brainstem and spinal cord, and its comparison with organotypic slice cultures. *Dev. Neurobiol.* **72**, 1140–1160.
- Davey G. E., Murmann P. and Heizmann C. W. (2001) Intracellular Ca<sup>2+</sup> and Zn<sup>2+</sup> levels regulate the alternative cell density-dependent secretion of S100B in human glioblastoma cells. *J. Biol. Chem.* **276**, 30819–30826.
- Donato R., Cannon B. R., Sorci G., Riuzzi F., Hsu K., Weber D. J. and Gezy C. L. (2013) Functions of S100 proteins. *Curr. Mol. Med.* **13**, 24–57.
- Ellis E. F., Willoughby K. A., Sparks S. A. and Chen T. (2007) S100B protein is released from rat neonatal neurons, astrocytes, and microglia by *in vitro* trauma and anti-S100 increases trauma-induced delayed neuronal injury and negates the protective effect of exogenous S100B on neurons. *J. Neurochem.* **6**, 1463–1470.
- Gentleman D. (1999) Improving outcome after traumatic brain injury—progress and challenges. *Br. Med. Bull.* **55**, 910–926.
- Kuzhandaivel A., Nistri A. and Mladinic M. (2010) Kainate-mediated excitotoxicity induces neuronal death in the rat spinal cord *in vitro* via a PARP-1 dependent cell death pathway (Parthanatos). *Cell. Mol. Neurobiol.* **30**, 1001–1012.
- Kuzhandaivel A., Nistri A., Mazzone G. L. and Mladinic M. (2011) Molecular mechanisms underlying cell death in spinal networks in relation to locomotor activity after acute injury *in vitro*. *Front. Cell. Neurosci.* **17**, 9.
- Kwon B. K., Stammers A. M., Belanger L. M. *et al.* (2010) Cerebrospinal fluid inflammatory cytokines and biomarkers of injury severity in acute human spinal cord injury. *J. Neurotrauma* **27**, 669–682.
- Margaryan G., Mattioli C., Mladinic M. and Nistri A. (2010) Neuroprotection of locomotor networks after experimental injury



- 1 to the neonatal rat spinal cord in vitro. *Neuroscience* **165**, 996–  
 2 1010.
- 3 Marquardt G., Setzer M., Theisen A., Tews D. S. and Seifert V. (2011)  
 4 Experimental subacute spinal cord compression: correlation of  
 5 serial S100B and NSE serum measurements, histopathological  
 6 changes, and outcome. *Neurol. Res.* **33**, 421–426.
- 7 Mazzone G. L. and Nistri A. (2010) Effect of the PARP-1 Inhibitor PJ 34  
 8 on excitotoxic damage evoked by kainate on rat spinal cord  
 9 organotypic slices. *Cell. Mol. Neurobiol.* **31**, 469–478.
- 10 Mazzone G. L. and Nistri A. (2011) Delayed neuroprotection by riluzole  
 11 against excitotoxic damage evoked by kainate on rat organotypic  
 12 spinal cord cultures. *Neuroscience* **190**, 318–327.
- 13 Mazzone G. L., Margaryan G., Kuzhandavil A., Nasrabad S. E.,  
 14 Mladinic M. and Nistri A. (2010) Kainate-induced delayed onset of  
 15 excitotoxicity with functional loss unrelated to the extent of  
 16 neuronal damage in the in vitro spinal cord. *Neuroscience* **168**,  
 17 451–462.
- 18 Mazzone G. L., Mladinic M. and Nistri A. (2013) Excitotoxic cell death  
 19 induces delayed proliferation of endogenous neuroprogenitor cells  
 20 in organotypic slice cultures of the rat spinal cord. *Cell Death. Dis.*  
 21 **4**, e902.
- 22 Mehta A., Prabhakar M., Kumar P., Deshmukh R. and Sharma P. L.  
 23 (2013) Excitotoxicity: bridge to various triggers in  
 24 neurodegenerative disorders. *Eur. J. Pharmacol.* **698**, 6–18.
- 25 Mercier E., Boutin A., Lauzier F. *et al.* (2013) Predictive value of  
 26 S-100 $\beta$  protein for prognosis in patients with moderate and severe  
 27 traumatic brain injury: systematic review and meta-analysis. *BMJ*  
 28 **346**, f1757.
- 29 Michetti F., Corvino V., Geloso M. C., Lattanzi W., Bernardini C.,  
 30 Serpero L. and Gazzolo D. (2012) The S100B protein in biological  
 31 fluids: more than a lifelong biomarker of brain distress. *J.*  
 32 *Neurochem.* **120**, 644–659.
- 33 Rammes A., Roth J., Goebeler M., Klempt M., Hartmann M. and Sorg  
 34 C. (1997) Myeloid-related protein (MRP) 8 and MRP14, calcium-  
 35 binding proteins of the S100 family, are secreted by activated  
 36 monocytes via a novel, tubulin-dependent pathway. *J. Biol. Chem.*  
 37 **272**, 9496–9502.
- 38 Rickmann M. and Wolff J. R. (1995) S100 protein expression in  
 39 subpopulations of neurons of rat brain. *Neuroscience* **67**, 977–991.
- 40 Rowland J. W., Hawryluk G. W., Kwon B. and Fehlings M. G. (2008)  
 41 Current status of acute spinal cord injury pathophysiology and  
 42 emerging therapies: promise on the horizon. *Neurosurg. Focus* **25**,  
 43 E2.
- 44 Roybon L., Lamas N. J., Garcia-Diaz A. *et al.* (2013) Human stem cell-  
 45 derived spinal cord astrocytes with defined mature or reactive  
 46 phenotypes. *Cell Rep.* **4**, 1035–1048.
- 47 Schwab J. M., Brechtel K., Mueller C. A., Failli V., Kaps H. P., Tuli S.  
 48 K. and Schluesener H. J. (2006) Experimental strategies to promote  
 49 spinal cord regeneration-an integrative perspective. *Prog. Neurobiol.*  
 50 **78**, 91–116.
- 51 Sorci G., Agneletti A. L., Bianchi R. and Donato R. (1998) Association  
 52 of S100B with intermediate filaments and microtubules in glial  
 53 cells. *Biochim. Biophys. Acta* **1448**, 277–289.
- 54 Sorci G., Riuzzi F., Arcuri C., Tubaro C., Bianchi R., Giambanco I. and  
 Donato R. (2013) S100B protein in tissue development, repair and  
 regeneration. *World J. Biol. Chem.* **4**, 1–12.
- Spenger C., Braschler U. F., Streit J. and Luscher H. R. (1991) An  
 organotypic spinal cord - dorsal root ganglion - skeletal muscle  
 coculture of embryonic rat. I. The morphological correlates of the  
 spinal reflex arc. *Eur. J. Neurosci.* **3**, 1037–1053.
- Streit J., Spenger C. and Luscher H. R. (1991) An organotypic spinal  
 cord - dorsal root ganglion - skeletal muscle coculture of  
 embryonic rat. II. Functional evidence for the formation of spinal  
 reflex arcs in vitro. *Eur. J. Neurosci.* **3**, 1054–1068.
- Wang Y. F. and Hatton G. I. (2009) Astrocytic plasticity and patterned  
 oxytocin neuronal activity: dynamic interactions. *J. Neurosci.* **29**,  
 1743–1754.
- Yokobori S., Hosein K., Burks S., Sharma I., Gajavelli S. and Bullock R.  
 (2013) Biomarkers for the clinical differential diagnosis in traumatic  
 brain injury-a systematic review. *CNS Neurosci. Ther.* **19**, 556–565.

# Graphical Abstract

The contents of this page will be used as part of the graphical abstract of html only. It will not be published as part of main article.



Excitotoxicity is a major mechanism responsible for neuronal death following acute spinal cord injury. The calcium-binding protein S100 $\beta$  is released by astrocytes into the extracellular compartment during the first 24 h after the initial insult and **1** represents a useful biomarker of lesion progression as its level is related to the occurrence and severity of neuronal loss.

# Author Query Form









Journal: JNC

Article: 12748

Dear Author,

During the copy-editing of your paper, the following queries arose. Please respond to these by marking up your proofs with the necessary changes/additions. Please write your answers on the query sheet if there is insufficient space on the page proofs. Please write clearly and follow the conventions shown on the attached corrections sheet. If returning the proof by fax do not write too close to the paper's edge. Please remember that illegible mark-ups may delay publication.

Many thanks for your assistance.

Query reference	Query	Remarks
1	<b>AUTHOR: Please check and confirm that the graphical abstract is fine for publication.</b>	
2	<b>AUTHOR: As per journal style, abbreviation [SDS] mentioned less than three times in the article is expanded in full. If expansion incorrect, please insert correct expansion.</b>	
3	<b>AUTHOR: Please provide 'room temperature' in degrees centigrade.</b>	
4	<b>AUTHOR: As per journal style, abbreviation [PBS] mentioned less than three times in the article is expanded in full. If expansion incorrect, please insert correct expansion.</b>	
5	<b>AUTHOR: As per journal style, abbreviation [HRP] mentioned less than three times in the article is expanded in full. If expansion incorrect, please insert correct expansion.</b>	
6	<b>AUTHOR: As per journal style, abbreviation [ECL] mentioned less than three times in the article is expanded in full. If expansion incorrect, please insert correct expansion.</b>	
7	<b>AUTHOR: Please give address information for Amersham Biosciences: town, state (if applicable), and country.</b>	
8	<b>AUTHOR: Gyorgy <i>et al.</i> 2011 has not been included in the Reference List, please supply full publication details.</b>	
9	<b>AUTHOR: Please define D-AVP.</b>	